IMPACT OF SWITCHING FUNCTIONS ON SLIDING MODE OBSERVER IN SENSORLESS PMSM DRIVES

Nguyen Khanh Quang[1]*, Nguyen Quang Linh[1], Le Phu Cuong[1], Hoang Than[2]

[1]*The University of Danang - University of Science and Technology, Danang, Vietnam*
[2]*Hue Industrial College, Hue, Vietnam*

*Corresponding author: nkquang@dut.udn.vn

(Received: May 08, 2025; Revised: June 15, 2025; Accepted: June 21, 2025)

DOI: 10.31130/ud-jst.2025.23(9B).507E

Abstract - The Sliding Mode Observer (SMO) algorithm has emerged as a promising solution for estimating the position and speed of motors, effectively replacing traditional physical sensors. This paper focuses on investigating the impact of switching functions in SMO on the control performance of Permanent Magnet Synchronous Motors (PMSMs) under the Field-Oriented Control (FOC) strategy. Through simulations conducted in Matlab/Simulink, the study evaluates the performance of SMO using three types of switching functions: Signum, Sigmoid, and Hyperbolic Tangent (Tanh). The results indicate that the Signum function induces chattering, significantly degrading system stability and accuracy. In contrast, the Sigmoid and Tanh functions deliver superior performance, with the Tanh function achieving the most optimal results. These findings provide a solid foundation for selecting appropriate switching functions to optimize SMO in sensorless PMSM control, while also opening new prospects for minimizing estimation errors and enhancing system responsiveness.

Key words - PMSM; SMO; FOC; Chattering; Sensorless.

1. Introduction

The rapid development of electric vehicle systems and industrial applications, Permanent Magnet Synchronous Motors (PMSMs) have emerged as a leading choice, gradually replacing induction motors in many modern drive systems due to their outstanding advantages such as high-power density, impressive energy efficiency, and precise controllability [1–5]. With these benefits, PMSMs have been widely applied in fields such as electric vehicles, household appliances, industrial machinery, and high-performance drive systems. However, conventional PMSM systems primarily rely on physical sensors to measure and feedback rotor speed and angular position for control purposes [6–10]. The use of these sensors introduces several challenges, including increased cost, added system weight, reduced reliability, and susceptibility to environmental noise. These limitations have driven the development of sensorless control methods, aiming to eliminate mechanical sensors while maintaining system performance. Among current sensorless control techniques, the Sliding Mode Observer (SMO) has emerged as a promising solution due to its ability to accurately and reliably estimate key parameters such as rotor position and speed without the use of physical sensors. Moreover, SMO exhibits strong noise immunity and is less sensitive to parameter variations, making it an ideal candidate for sensorless PMSM control. However, the most significant drawback of SMO lies in the high-frequency chattering phenomenon, which stems from the use of discontinuous switching functions such as the Signum function. Chattering not only introduces noise but also degrades estimation accuracy and induces harmonic distortion in the control system, ultimately affecting overall system quality. To address the chattering issue, several solutions have been proposed in previous studies, including the integration of Phase-Locked Loops (PLL), the use of Kalman filters [11-12], and the replacement of switching functions with fuzzy logic techniques [6–12]. While these methods help reduce chattering, they often come with drawbacks such as reduced dynamic response or increased algorithmic complexity. Therefore, optimizing the switching function in SMO to achieve a balance between accuracy and performance without increasing complexity is essential. This study focuses on evaluating the impact of continuous switching functions, such as the Sigmoid and Hyperbolic Tangent (Tanh) functions, as alternatives to the traditional Signum function in SMO. The goal is to improve the performance of sensorless PMSM control systems, reduce chattering, and enhance estimation accuracy. Through simulation scenarios in Matlab/Simulink, the study investigates and compares these switching functions in terms of their effectiveness in optimizing the control system. The remainder of this paper is organized as follows: Section 2 presents the theoretical background of PMSM and the SMO algorithm. Section 3 analyzes the characteristics of different switching functions used in the observer. Simulation results and detailed evaluations are provided in Section 4. Finally, Section 5 concludes the paper and suggests directions for future research.

2. Mathematical Model of the PMSM and the Sliding Mode Observer Algorithm

In the $\alpha-\beta$ coordinate system, the PMSM is described by the following equations:

$$\begin{cases} L_s \dfrac{d}{dt}(i_\alpha) = -R_s i_\alpha - e_\alpha + V_\alpha \\ L_s \dfrac{d}{dt}(i_\beta) = -R_s i_\beta - e_\beta + V_\beta \end{cases} \quad (1)$$

where: R_s and L_s are the stator resistance and inductance, respectively; i_α, i_β, V_α, V_β are the stator currents and voltages, respectively; e_α and e_β are the back EMFs whose values are given by equation (2):

$$\begin{cases} e_\alpha = -\lambda_m \omega_r \cos\theta_r \\ e_\beta = -\lambda_m \omega_r \sin\theta_r \end{cases} \quad (2)$$

The sliding mode observer is designed as follows [9]:

$$\begin{cases} L_s \dfrac{d}{dt}(\hat{i}_\alpha) = -R_s \hat{i}_\alpha - kSF(\hat{i}_\alpha - i_\alpha) + V_\alpha \\ L_s \dfrac{d}{dt}(\hat{i}_\beta) = -R_s \hat{i}_\beta - kSF(\hat{i}_\beta - i_\beta) + V_\beta \end{cases} \quad (3)$$

where k is the sliding mode observer gain ($k > 0$) and SF is the switching function. By subtracting equation (3) from equation (1), it can be observed that V_α and V_β are canceled out, and the error equation becomes:

$$\begin{cases} L_s \dfrac{d}{dt}(\tilde{i}_\alpha) = -R_s \tilde{i}_\alpha - kSF(\tilde{i}_\alpha) + e_\alpha \\ L_s \dfrac{d}{dt}(\tilde{i}_\alpha) = -R_s \tilde{i}_\beta - kSF(\tilde{i}_\beta) + e_\beta \end{cases} \quad (4)$$

When the sliding observer reaches the sliding surface, the error values $\tilde{i}_\alpha$ and $\tilde{i}_\beta$ will approach 0. At that point, from equation (4), we obtain the estimated values of the electromotive force (EMF):

$$\begin{cases} \hat{e}_\alpha = kSF(\tilde{i}_\alpha) \\ \hat{e}_\beta = kSF(\tilde{i}_\beta) \end{cases} \quad (5)$$

Apply a low-pass filter to these values to eliminate higher-order harmonic components, while compensating for the phase delay caused by the filter:

$$\begin{cases} \hat{e}_{s\alpha} = \dfrac{\omega_c}{\omega_c + s} \hat{e}_\alpha \\ \hat{e}_{s\beta} = \dfrac{\omega_c}{\omega_c + s} \hat{e}_\beta \end{cases} \quad (6)$$

with $\omega_c = 2\pi f_c$, f_c is the cutoff frequency of the filter. Regarding the role of the LPF, a smaller cutoff frequency f_c results in better signal smoothing and reduced chattering but increases phase delay, leading to errors in position and speed estimation, particularly at high speeds. This can degrade the performance of Field-Oriented Control (FOC). Conversely, a larger f_c reduces phase delay, improving dynamic response, but may fail to filter out all high-frequency components, resulting in residual chattering, especially when using the Signum function.

The position and speed of the rotor can be estimated using the following equation:

$$\begin{cases} \hat{\theta} = \arctan\left(-\dfrac{\hat{e}_{s\alpha}}{\hat{e}_{s\beta}}\right) + \Delta\theta \\ \hat{\omega}_r = \dfrac{d\hat{\theta}}{dt} \end{cases} \quad (7)$$

Through the equations from (1) to (7), the basic block diagram of the sliding observer is shown in Figure 1.

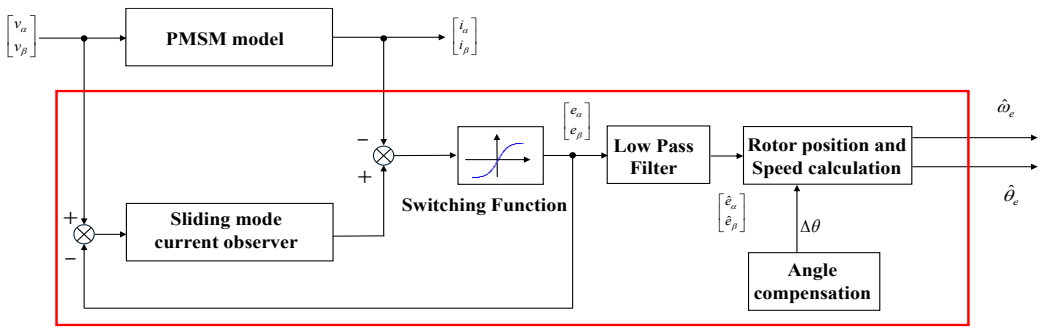

Figure 1. *The architecture of the SMO [9]*

3. Characteristics of the Switching Functions in SMO

In the SMO block diagram presented in Figure 1, the switching function helps the system maintain the sliding surface in the state space, allowing the observer to quickly respond to changes in internal parameters or external disturbances. For traditional sliding observers, the Signum function (denoted: sgn(x)) is commonly used in SF. This function has a simple structure, quick response capability, and is defined by the following equation:

$$\text{sgn}(x) = \begin{cases} 1 & x > 0 \\ 0 & x = 0 \\ -1 & x < 0 \end{cases} \quad (8)$$

The use of the function sign(x) in SMO comes with some notable drawbacks, particularly the chattering phenomenon. The characteristic of the Signum function is its immediate response to small changes in the system's state, leading to continuous oscillations between positive and negative values. The sudden transition from -1 to 1 when the input crosses the zero threshold generates large control impulses, causing the system to struggle to stay on the sliding surface. The chattering phenomenon not only negatively affects control performance but also increases energy consumption and causes wear on mechanical components, thereby reducing the reliability and lifespan of the system.

The Sigmoid and Tanh functions are mathematically described in equations (9) and (10), respectively.

$$\sigma(x) = \frac{1}{1 + e^{-\mu x}} \quad (9)$$

$$\tanh(x) = \frac{e^{\mu x} - e^{-\mu x}}{e^{\mu x} + e^{-\mu x}} \quad (10)$$

where μ is the shaping coefficient. By adjusting the shaping parameters will adjust the slope of the function at

the central point. Specifically, a larger μ value increases the slope, enabling the system to respond faster to small deviations, but it may increase the risk of oscillations if too large. Conversely, a smaller μ value reduces the slope, making the system smoother but potentially slowing down the convergence speed. In the paper, we used the standard forms of the Sigmoid function and Tanh function with $\mu = 1$ to simplify simulations and focus on comparing the fundamental characteristics of these functions. The paper proposes using these two functions as an alternative to the Signum function, due to their ability to create smooth transitions between the system's states, thus minimizing the chattering phenomenon. The main difference between these two functions is their range of values: the Sigmoid function is limited to the range (0, 1), while the Tanh function extends from (-1, 1). This difference allows Tanh to reflect both positive and negative directions, making it the optimal choice for applications requiring flexible feedback. Furthermore, Tanh has a larger slope at the center point, enabling it to respond more sensitively to small changes, thereby improving the system's control performance. Figure 2 illustrates the shapes of the Signum, Sigmoid, and Tanh functions.

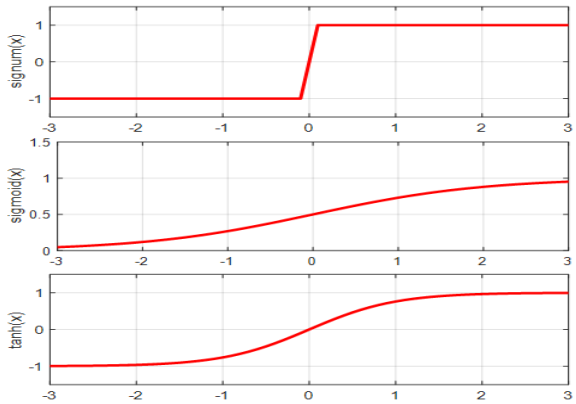

Figure 2. *Various types of switching functions: Signum, Sigmoid, and Hyperbolic*

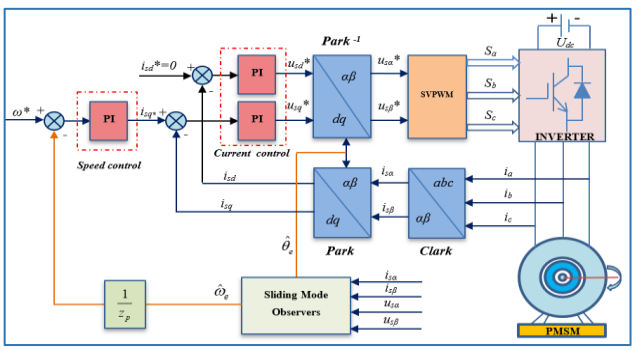

Figure 3. *Simulation model of sensorless PMSM motor control*

4. Characteristics of the Switching Functions in SMO

The block diagram illustrating the sensorless control of the PMSM based on SMO is developed using MATLAB Simulink, as presented in Figure 3. The control architecture consists of two key loops: the current control loop and the speed control loop. The SMO receives input in the $\alpha - \beta$ coordinate system, which is derived from the $a - b - c$ coordinate system via the Clarke transformation block. The SMO's output provides critical information regarding the rotor's position and speed, which is then utilized for closed-loop control. A Proportional-Integral (PI) controller is applied in both loops, incorporating the coordinate transformation to generate the required control signals, which are subsequently fed to the motor through the Space Vector Pulse Width Modulation (SVPWM) inverter control module. The necessary simulation parameters for the PMSM motor, which are detailed in Table 1, are used to configure the model.

In order to accurately simulate and assess the impact of the transformation functions in the SMO, this study maintains the original parameters while varying the SF functions across three scenarios:

- Scenario 1 (S1): Signum function
- Scenario 2 (S2): Sigmoid function
- Scenario 3 (S3): Tanh function.

Table 1. *PMSM Motor Parameters*

Parameters	Value
Stator phase resistance R_s (Ω)	2.875
Direct axis inductance L_d (mH)	8.5
Quadrature axis inductance L_q (mH)	8.5
Flux linkage from rotor λ_m (Wb)	0.175
Moment of inertia J $(kg.m^2)$	0.001
Number of pole pairs n_p $(-)$	4

The initial speed command is set to 300 rpm from 0 to 0.3 seconds, then increases to 500 rpm and remains stable until 0.5 seconds. Figure 4 presents a comparison of rotor speed waveforms across three different scenarios. It is clear that the estimated rotor speed closely matches the actual speed. As seen in Figure 4(a), the traditional SMO control method using the Signum function is effective in estimating the desired speed. Once the system reaches a steady state, the estimated speed aligns well with the actual speed. However, there is significant chatter during the speed transition, causing noticeable deviation in the estimated value. The time required to reach a steady state is relatively long (45 ms). Although some overshoots are observed during the initial control phase and when the speed command changes, the effect of chatter has been significantly reduced, and the system stabilizes quickly in a short time when using the two alternative SF functions, sigmoid and Tanh (S2: 20 ms; S3: 15 ms). The speed response becomes noticeably "smoother", indicating that the estimated speed better tracks the set speed and converges to the actual speed, demonstrating that the SMO system performs more effectively in Figure 4 (b) with SMO using Tanh. Figure 5 shows the flux angle curves of the motor. It can be observed that the estimated flux angle maintains good "tracking" with the actual angle, indicating that the estimation capability of SMO is very effective. In Figure 4, the estimated flux angle is delayed compared to the actual angle (59 µs), which leads to an error affecting the system's angle feedback performance. This phenomenon is due to the influence of

the Low Pass Filter (LPF) and the Switch Function (SF). After changing the conversion function from Signum to Sigmoid and Tanh, the estimated angle still lags the actual angle but with a shorter delay time (S2: 54 µs; S3: 18 µs). Moreover, the use of these functions not only reduces the delay but also significantly diminishes the chattering effect. We observe that applying the functions in S2 and S3 to the sliding mode observer has a better effect on the flux angle estimation results, improving both the accuracy and stability of the system.

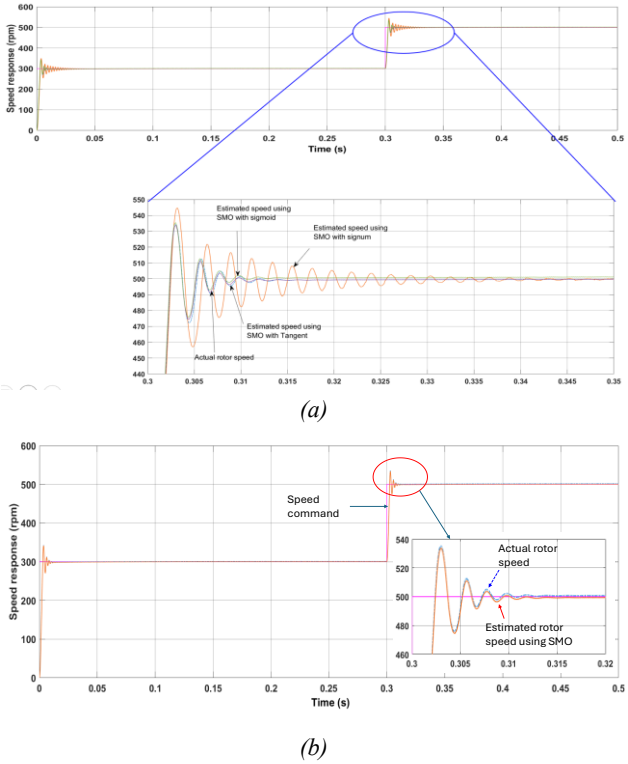

Figure 4. *A comparison of rotor speed*

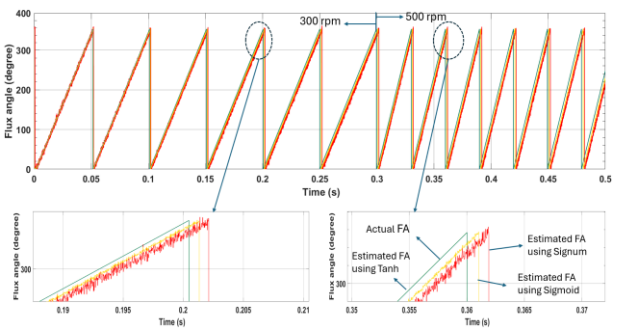

Figure 5. *Comparison of the rotor position estimation using SMO with the difference SF*

5. Conclusion

This study has investigated the impact of switching functions in the Sliding Mode Observer algorithm. The results clearly demonstrate that the choice of switching function plays a crucial role in determining the performance of PMSM motor control. While the Signum function leads to significant chattering, thereby compromising accuracy, both the Tanh and Sigmoid functions exhibit superior performance, with the Tanh function delivering the most optimal results. These findings provide a comprehensive foundation for selecting the most appropriate switching function to optimize the performance of SMO in sensorless PMSM motor control systems. Furthermore, they open new avenues for enhancing error reduction and improving system responsiveness. Future studies should explore additional switching functions and incorporate advanced optimization algorithms to further elevate the performance, robustness, and stability of the motor control systems.

Acknowledgments: This work was supported by The University of Danang - University of Science and Technology, code number of Project: T2025-02-04.

REFERENCES

[1] D. Fu, X. Zhao, and J. Zhu, "A Novel Robust Super-Twisting Nonsingular Terminal Sliding Mode Controller for Permanent Magnet Linear Synchronous Motors", *IEEE Transactions on Power Electronics*, vol. 37, no. 3, pp. 2936-2945, 2022. doi: 10.1109/TPEL.2021.3119029.

[2] J. Zhang *et al*., "Novel Dynamic Microactuation Method for Tracking-Error Reduction of Permanent Magnet Linear Synchronous Motors", *IEEE Transactions on Industrial Electronics*, vol. 69, no. 9, pp. 9165-9175, 2022. doi: 10.1109/TIE.2021.3115632.

[3] Y. S. Kung, N. K. Quang, and L. T. Van Anh, "FPGA-based neural fuzzy controller design for PMLSM drive", *2009 International Conference on Power Electronics and Drive Systems (PEDS)*, Taipei, Taiwan, 2009, pp. 222-227.

[4] V. Q. B. Ngo, N. K. Anh, and N. K. Quang, "FPGA-Based Adaptive PID Controller Using MLP Neural Network for Tracking Motion Systems", *IEEE Access*, vol. 12, pp. 91568-91574, 2024. doi: 10.1109/ACCESS.2024.3422015.

[5] L. Xiong, X. Liu, L. Liu, and Y. Liu, "Amplitude-Phase Detection for Power Converters Tied to Unbalanced Grids with Large X/R Ratios", *IEEE Transactions on Power Electronics*, vol. 37, no. 2, pp. 2100-2112112, 2022oi: 10.1109/TPEL.2021.3104591.

[6] Y. Zhao, M. Feng, and W. Li, "Improved Rotor Position Detection Method Based on SMO", *J. Beijing Univ. Aeronautics Astronautics*, vol 46, no.12, pp. 2329–2338, 2020. doi: 10.13700/j.bh.1001-5965.2019.0637

[7] C. Mingxia and Z. Yuguang, "Simulation Research on Sensorless Speed Control System of Permanent Magnet Synchronous Motor Based on SMO", *2016 Eighth International Conference on Measuring Technology and Mechatronics Automation* (ICMTMA), Macau, China, 2016, pp. 610-613.

[8] Mahmoud M. Gaballah, Mohammad El Bardini and Mohammad Sharaf, "Chattering-free sliding mode observer for speed sensorless control of PMSM", *Applied Computing and Informatics*, vol 13, pp. 169-174, 2017.

[9] N. K. Quang, D. Q. Vinh, N. That, and Q. P. Ha, "Observer-based integral sliding mode control for sensorless PMSM drives using FPGA", *International Conference on Control, Automation and information Sciences (ICCAIS)*, Nha Trang, Vietnam, 2013, pp. 218–223.

[10] A. Farahat, Z. Liu, G. Liu, and Q. Chen, "Speed and Position Estimation for 5-ph PMSM Using SOGI Based on SMO Considering Short-Circuit Fault", *IEEE Access*, vol. 12, pp. 57315-57325, 2024. doi: 10.1109/ACCESS.2024.3387284.

[11] A. H. T A and V. G, "Sensorless Speed Control of PMSM Based on SMO with Traditional PLL and Tangent Function PLL", *2024 IEEE International Conference on Smart Power Control and Renewable Energy (ICSPCRE)*, Rourkela, India, 2024, pp. 1-5.

[12] K. Yu, S. Li, W. Zhu, and Z. Wang, "Sensorless Control Scheme for PMSM Drive via Generalized Proportional Integral Observers and Kalman Filter", *IEEE Transactions on Power Electronics*, vol. 40, no. 3, pp. 4020-4033, 2025. Doi: 10.1109/TPEL.2024.3502396.